Food Chemistry 384 (2022) 132581

Contents lists available at ScienceDirect

Food Chemistry

journal homepage: www.elsevier.com/locate/foodchem

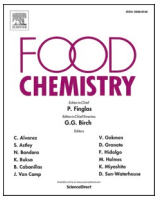

The effect of Holder pasteurization on the lipid and metabolite composition of human milk

Isabel Ten-Doménech [a,1], Victoria Ramos-Garcia [a,1], Marta Moreno-Torres [b], Anna Parra-Llorca [a], María Gormaz [a,c], Máximo Vento [a,c], Julia Kuligowski [a,*], Guillermo Quintás [d,e]

[a] Neonatal Research Group, Health Research Institute Hospital La Fe, Avda Fernando Abril Martorell 106, 46026 Valencia, Spain
[b] Unidad de Hepatología Experimental, Health Research Institute Hospital La Fe, Avda Fernando Abril Martorell 106, 46026 Valencia, Spain
[c] Division of Neonatology, University & Polytechnic Hospital La Fe, Avda Fernando Abril Martorell 106, 46026 Valencia, Spain
[d] Health and Biomedicine, Leitat Technological Center, Carrer de la Innovació 2, 08225 Terrassa, Spain
[e] Analytical Unit, Health Research Institute La Fe, Avda Fernando Abril Martorell 106, 46026 Valencia, Spain

ARTICLE INFO

Keywords:
Donor human milk
Holder pasteurization
Preterm infant
Metabolomics
Lipidomics
Network analysis

ABSTRACT

Human milk (HM) is the gold standard for newborn nutrition. When own mother's milk is not sufficiently available, pasteurized donor human milk becomes a valuable alternative. In this study we analyzed the impact of Holder pasteurization (HoP) on the metabolic and lipidomic composition of HM. Metabolomic and lipidomic profiles of twelve paired HM samples were analysed before and after HoP by liquid chromatography–mass spectrometry (MS) and gas chromatography-MS. Lipidomic analysis enabled the annotation of 786 features in HM out of which 289 were significantly altered upon pasteurization. Fatty acid analysis showed a significant decrease of 22 out of 29 detectable fatty acids. The observed changes were associated to five metabolic pathways. Lipid ontology enrichment analysis provided insight into the effect of pasteurization on physical and chemical properties, cellular components, and functions. Future research should focus on nutritional and/or developmental consequences of these changes.

1. Introduction

Human milk (HM) is the gold standard for infant nutrition and provides the optimum composition of nutritional elements needed for growth and development. Consequently, HM offers numerous short and long-term benefits to the infant-mother dyad (World Health Organization, 2017). Of note, the survival of extremely low gestational age newborns has consistently improved in the last decades (Boquien, 2018). In this scenario, early infant nutrition has become a major player in improving clinical outcomes of survivors and based on an impressive array of benefits, HM is the first choice for feeding preterm infants (Miller et al., 2018).

When own mother's milk (OMM) renders insufficient, pasteurized donor human milk (DHM) rather than preterm infant formula is the preferred alternative for preterm infants (Poulimeneas et al., 2021). The use of DHM in comparison to the use of formula milk might reduce the incidence of necrotizing enterocolitis (Miller et al., 2018; Quigley, Embleton, & McGuire, 2019), and although it has been linked to lower rates of weight gain, linear growth, and head growth during hospital admission, no differences in long term growth have been described (Quigley et al., 2019). The exclusive feeding of pasteurized DHM undoubtedly has an impact on different aspects of preterm biology. Hence, DHM modifies the gut-microbiota composition of preterm infants as compared to the use of OMM (Parra-Llorca et al., 2018), although it does not compromise the protection against oxidative stress (Parra-Llorca et al., 2019). Furthermore, preterm infants exclusively receiving DHM exhibited different urinary steroid hormone levels when compared to infants receiving OMM. These findings might be potentially linked to steroid hormone concentrations present in fresh and pasteurized HM (Piñeiro-Ramos et al., 2021).

The composition of HM is affected by processing and handling of expressed HM following stringent protocols applied in HM banks involving pasteurization, necessary for minimizing the potential to transmit infectious agents, as well as freezing, long-term storage, and multiple container passages (Colaizy, 2021). Low-temperature (62.5 °C) long-time (30 min) pasteurization known as "Holder" pasteurization

* Corresponding author.
E-mail address: Julia.kuligowski@uv.es (J. Kuligowski).
[1] Both authors contributed equally.

https://doi.org/10.1016/j.foodchem.2022.132581
Received 14 October 2021; Received in revised form 4 February 2022; Accepted 25 February 2022
Available online 26 February 2022

(HoP) is routinely employed at HM banks to avoid newborn infection through transmission of pathogens that might be present in DHM as it destroys vegetative forms of bacteria and most viruses including human immunodeficiency virus, herpes, and cytomegalovirus (Colaizy, 2021). The use of softer alternatives (e.g., high-temperature short-time, high pressure processing, ultraviolet and microwave irradiation, and thermosonic processing (Wesolowska et al., 2019) has been in the spotlight of on-going investigations. However, to our knowledge, none of these techniques has been yet implemented for the routine processing of small volume milk batches (approximately 3–6 L) at HM banks.

While total carbohydrates and proteins contents remain relatively stable upon HoP, there is controversy regarding the degree of loss of total fat, as percentages between −6.2 and −25% have been reported in studies replicating current milk bank procedures (Colaizy, 2021). Furthermore, several bioactive components, such as enzymes, immunoglobulins, cytokines, microRNAs, and immune cells are inactivated or destroyed (Wesolowska et al., 2019). Scientific evidence documenting the effects of HoP on changes of specific lipid and metabolite classes is scant. The present study aims at the characterization of the impact of HoP on the global HM metabolome and lipidome. Metabolomic and lipidomic profiles of twelve paired HM samples collected before and after HoP were analyzed by liquid chromatography–high resolution mass spectrometry (LC-HRMS) and gas chromatography-MS (GC–MS). Results obtained enabled the identification of potentially relevant alterations at the metabolic pathway level. Finally, the potential implications of the observed compositional changes in the properties and functionality of HM are discussed.

2. Material and methods

2.1. Human milk samples

The study was conducted in accordance with relevant guidelines and regulations including the Declaration of Helsinki. The Ethics Committee for Biomedical Research of the Health Research Institute La Fe (Valencia, Spain) approved the study protocol (approval number 2014/0247), and mothers gave their written consent to participate. DHM (N = 12) samples were provided by healthy HM donors admitted after routine screening and interview to the HM bank at the University and Polytechnic Hospital La Fe (Valencia, Spain). The median gestational age at which milk donors had given birth was 40 (interquartile range, IQR = 4) weeks. Milk expression was accomplished with breast milk pumps following the standard operating procedure routinely employed at the hospital and the HM bank. Prior to extraction, removable parts of the breast milk pump and collection bottles were sterilized. In addition, mothers washed their hands with soap and water, and their nipples with water. After extraction, bottles were stored at −20 °C. Milk bottles from the same mother were defrosted and pooled together to form a batch of approximately 2 L and after gentle shaking, a 1 mL aliquot of it was collected in a dry, 1.5 mL microcentrifuge tube before and after HoP (30 min at 62.5 °C followed by fast cooling to 4 °C). The median elapsed time between the first and last expression of a pooled DHM sample was 25 (IQR = 36) days. Time of collection in relation to the infants' age was established from this median value and ranged between 21 and 164 days after delivery with a median value of 87 days (IQR = 83).

2.2. Lipidomic and metabolomic analyses of HM samples

Standards and reagents. LC-MS grade acetonitrile (CH_3CN), methanol (CH_3OH), *n*-hexane (>98%), and isopropanol (IPA), reagent grade methyl *tert*-butyl ether (MTBE), ammonium acetate (≥98%), formic acid (HCOOH, >98%), methanolic HCl (3 N), Supelco 37-component fatty acid methyl ester (FAME) mix, lauric acid-D_{23} (≥98%), and nonadecanoic acid (≥98%), were obtained from Merck Life Science S.L. U. (Madrid, Spain). Ultra-pure water (>18.2 MΩ) was generated using a Milli-Q Water Purification System (Merck Millipore, Darmstadt, Germany). (15,15,16,16,17,17,18,18,18-D_9) oleic acid-D_9 (>99%) was purchased from Avanti Polar Lipids (Alabaster, AL, USA) and prostaglandin $F_{2\alpha}$-D_4 (≥98 %, deuterated incorporation ≥ 99%) was purchased from Cayman Chemical Company (Ann Arbor, MI, USA).

HM untargeted metabolomic and lipidomic analyses. HM samples were thawed at room temperature and then heated in a water bath for 10 min at 33 °C. 5 μL of an internal standard (IS) solution containing oleic acid-D_9 (80 μM) and prostaglandin F2α-D_4 (39 μM) in H_2O were added to 45 μL of HM. A single-phase extraction procedure adding 175 μL of CH_3OH and 175 μL of MTBE (Villaseñor et al., 2014) to each HM sample followed by a 4 fold dilution of the supernatant with a CH_3OH:MTBE (1:1, v/v) solution was applied. The resulting extract was used for both lipidomic and metabolomic analyses. In addition, a blank extract was prepared following the steps described for HM samples but replacing HM with water. A pooled quality control (QC) sample was prepared by mixing 20 μL of each HM sample extract.

For untargeted lipidomic and metabolomic analysis, a 1290 Infinity ultra-performance LC (UPLC) system coupled to a 6550 Spectrometer iFunnel quadrupole time-of-flight (QqTOF) MS system from Agilent Technologies (Santa Clara, CA, USA) was used. A detailed description of the parameters used for lipidomic fingerprinting of HM samples can be found elsewhere (Horta et al., 2020; Ten-Doménech et al., 2020). In short, an Acquity BEH C18 column (50 × 2.1 mm, 1.7 μm) from Waters (Milford, MA, USA) running a binary mobile phase gradient with (5:1:4 IPA:CH_3OH:H_2O 5 mM CH_3COONH_4, 0.1% v/v HCOOH) and (99:1 IPA:H_2O 5 mM CH_3COONH_4, 0.1% v/v HCOOH) as mobile phase components was used. Column and autosampler were kept at 55 and 4 °C, respectively, the flow rate was 0.4 mL min^{-1}, and the injection volume was 2 μL. For untargeted metabolomics screening of HM extracts, a Synergi^{TM} Hydro-RP 80 Å LC C18 column (150 × 2 mm, 4 μm) from Phenomenex (Torrance, CA, USA) employing a stepwise gradient with solvent A (H_2O, 0.1% v/v HCOOH) and solvent B (CH_3CN, 0.1% v/v/HCOOH) as mobile phase components was used as follows: 1% B was held for 2 min followed by a linear gradient from 1 to 80% B in 8 min and from 80 to 98% B in 0.1 min; 98% B were held for 1.9 min before returning to initial conditions in 0.1 min and column equilibration with 1% B during 2.9 min. The flow rate was set to 0.4 mL min^{-1}, column and autosampler to 40 and 4 °C, respectively, and the injection volume was 3 μL.

MS detection was carried out in the ESI^+ mode (lipidomics) and the ESI^+ and ESI^- modes (metabolomics). Full scan MS data was acquired between 70 and 1500 *m/z* using the following ionization parameters: gas T, 200 °C; drying gas, 14 L min^{-1}; nebulizer, 37 psi; sheath gas T, 350 °C; sheath gas flow, 11 L min^{-1}. Mass reference standards were introduced into the source for automatic MS spectra recalibration during analysis via a reference sprayer valve using the 149.02332 (background contaminant), 121.050873 (purine), and 922.009798 (HP-0921) *m/z* as references in ESI^+ and 119.036 (purine) and 980.0163 ([HP-0921 + CH_3COOH-H]-) *m/z* in ESI^-. MS^2 data were acquired using data dependent acquisition methods as explained elsewhere (Ten-Doménech et al., 2020) using centroid mode at a rate of 5 Hz in the extended dynamic range mode (2 GHz), a collision energy set to 20 V, medium isolation window (~4 amu), MS^2 fragmentation with automated selection of five precursor ions per cycle, and an exclusion window of 0.15 min after two consecutive selections of the same precursor. UPLC-QqTOF-MS data acquisition was carried out employing MassHunter Workstation (version B.07.00) from Agilent.

Before UPLC-QqTOF-MS experiments, a system suitability check was carried out by analyzing a 2 μM IS solution. Then, 2 blanks and several QCs (9 and 20 replicates for metabolomics and lipidomic analysis, respectively) were injected at the beginning of the sequence for system conditioning and MS^2 data acquisition. HM sample extracts were injected in random order. The QC was injected every six samples and twice at the beginning and end of the batch for assessment and correction of instrumental performance (Broadhurst et al., 2018). The blank extract was injected twice at the end of the measurement sequence to

identify signals from other than biological origin, and possible carry-over (Martínez-Sena et al., 2019).

Analysis of fatty acid methyl esters (FAMEs). The determination of 36 FAMEs was performed employing a previously described GC–MS method (Cruz-Hernandez, Goeuriot, Giuffrida, Thakkar, & Destaillats, 2013) with slight modifications. Briefly, a HM aliquot was defrosted on ice and gently shaken to avoid phase separation. Then, 250 μL of HM and 600 μL of *n*-hexane containing ISs (12 μM lauric acid-D_{23} and 26 μM nonadecanoic acid) were mixed in a 15 mL test tube equipped with Teflon-lined screw caps. An aliquot of 2 mL of CH_3OH, 2 mL of CH_3OH /HCl (3 N), and 1 mL of *n*-hexane were added and vortexed vigorously. Derivatization was carried out in a water bath at 90 °C for 60 min, with occasional additional shaking. After cooling down to room temperature, 2 mL of water were added and shaken vigorously prior to centrifugation (1200 × *g* for 5 min at 4 °C). The upper hexane layer containing the extracted derivatives was transferred into GC–MS vials. GC–MS analysis was conducted using an Agilent 7890B GC system coupled to an Agilent 5977A quadrupole MS detector operating in selected ion monitoring (SIM) mode. Separations were performed using a Zebron™ ZB-WAX-plus™ column (30 m × 250 μm i.d., 0.25 μm film thickness, Phenomenex, Torrance, CA, USA). Two microliters of derivatives were injected in split mode with a ratio of 40:1, and the solvent delay time was set to 2.6 min. The initial oven temperature was held at 60 °C for 2 min, ramped to 150 °C at a rate of 13 °C min^{-1} and held for 15 min, and to 240 °C at a rate of 2 °C min^{-1} and held for 2 min. Helium was used as a carrier gas at a constant flow rate of 1 mL min^{-1} through the column. The temperatures of the front inlet, transfer line, and electron impact (EI) ion source were set at 250, 290, and 230 °C, respectively, and the electron energy was −70 eV. Further measurement parameters used for the studied analytes are summarized in Supplementary Table S1. For quantification, an external calibration line was employed using standard solutions obtained from different volumes of the Supelco 37-component FAME mix after evaporation and reconstitution in *n*-hexane containing derivatized IS compounds. This procedure was used to remove the 37-component FAME mix solvent (i.e., dichloromethane) and consequently, the most volatile FAME (i.e., FAME of butyric acid) was lost and could no longer be quantified.

The method was validated based on the US Food and Drug Administration (FDA) guidelines for bioanalytical method validation (Food and Drug Administration (FDA). Guidance for Industry: Bioanalytical Method Validation. Food and Drug Administration, Center for Drug Evaluation and Research, Center for Veterinary Medicine, 2018) including the following bioanalytical parameters: linearity range, selectivity and specificity, sensitivity, carry-over, accuracy, precision, recovery, and stability. The linear range was selected according to the expected concentrations ranges in HM samples. Calibration curves included a blank without analytes nor IS, a zero calibrator (i.e., blank with IS) and, at least, six standards covering the selected concentration ranges. Accuracy, precision, specificity, and recovery of the method were established from the replicate analysis (N = 3) of standards and spiked samples at three concentration levels (low, medium, and high) conducted on three different days to ensure that the extraction of the metabolites was efficient and reproducible. Selectivity and specificity were demonstrated by analyzing multiple blanks. Carry-over was assessed by the analysis of zero-injections after the analysis of high concentrated standards and spiked samples (N = 3). Autosampler and processed sample stability were assessed by comparing concentrations observed in a freshly prepared sample and in the same processed sample after 20 h stored in the autosampler (sealed vial, 25 °C). Analytes' freeze–thaw stability was established by comparing concentrations observed in a sample after three freeze–thaw cycles (−80 °C) to a freshly prepared sample.

2.3. Data processing and statistics

Lipidomics and metabolomics data pre-processing. Centroid UPLC-QqTOF-MS raw data were converted to mzXML format employing ProteoWizard (Kessner, Chambers, Burke, Agus, & Mallick, 2008) (http://proteowizard.sourceforge.net). XCMS software (http://metlin.scripps.edu/xcms/) (Tautenhahn, Patti, Rinehart, & Siuzdak, 2012) and CAMERA (Kuhl, Tautenhahn, Böttcher, Larson, & Neumann, 2012) in R 3.6.1 were employed for the generation of peak tables. Peak table extraction for lipidomics is described elsewhere (Ten-Doménech et al., 2020). The selection of parameters for peak table extraction and alignment for metabolomics was based on the observed variation of RT and *m/z* values of ISs. The centWave method with the following settings was used for peak detection: *m/z* range = 70–1500, ppm = 15, peakwidth = (5 and 20), snthr = 6, prefilter = (3, 100). A minimum difference in *m/z* of 0.01 Da was selected for overlapping peaks. Intensity-weighted *m/z* values of each feature were calculated using the wMean function. Peak limits used for integration were found through descent on the Mexican hat filtered data. Peak grouping was carried out using the "density" method using mzwid = 0.015 and bw = 5. RT correction was carried out using the "obiwarp" method. After peak grouping, the fillPeaks method with the default parameters was applied to fill missing peak data. Automatic integration was assessed by comparison to manual integration using IS signals. A total of 18401 (lipidomic analysis), 1826 (metabolomic analysis, ESI^+) and 893 (metabolomic analysis, ESI^-) features were initially detected after peak detection, integration, chromatographic deconvolution, and alignment in HM samples.

Further data processing and statistical analysis were carried out in MATLAB 2019b (Mathworks Inc., Natick, MA, USA) using in-house written scripts available from the authors, and the PLS Toolbox 8.7 (Eigenvector Research Inc., Wenatchee, USA). Data were annotated by automatic matching of experimental MS^2 spectra to publicly available databases (i.e., HMDB, MS-DIAL, and LipidBlast) as described elsewhere (Ten-Doménech et al., 2020). In addition, Lipidex (Hutchins, Russell, & Coon, 2018) was used for the annotation of lipidomic data (mass error 20 ppm). Enlargement of metabolite annotation was achieved with the Metabolic reaction network-based recursive algorithm (MetDNA) (Shen et al., 2019).

Intra-batch effect correction was performed using the Quality Control-Support Vector Regression algorithm employing a Radial Basis Function kernel (Kuligowski, Sánchez-Illana, Sanjuán-Herráez, Vento, & Quintás, 2015) and the LIBSVM library (Chang & Lin, 2011) with the following parameters: ε–range = 2 to 5%; γ-range = 1 to 10^5; C = 90%. Features with RSD (QC) > 20% after QC-SVRC, and those for which the ratio between the median peak area values in QCs and blanks was lower than a threshold value (i.e., 9 and 3 in metabolomic and lipidomic experiments, respectively) were classified as unreliable and removed from further analysis.

Network-based analysis. Differences between HM before and after pasteurization on the pathway level were studied employing the "Functional Analysis" tool (version 2.0) available in MetaboAnalyst 5.0 (Chong et al., 2018) using a mass accuracy of 10 ppm, the *mummichog* algorithm with a *p*-value cut-off of 0.005, and the Kyoto Encyclopedia of Genes and Genomes (KEGG) *Homo Sapiens* pathway library (Caspi et al., 2016). *Mummichog* analysis was carried out using the *m/z* and RT values of each feature and the FDR-corrected *p*-values from a *t*-test to test whether the unknown population means of the two groups were equal, accounting for unequal variances. Using the results of the *mummichog* algorithm, matched compounds (i.e., hits) were assigned to their corresponding *m/z*-RT features of the dataset. Then, KEGG compounds and KEGG glycans of each significantly altered pathway were searched in the matched *mummichog* compound list and assigned to unique features in the dataset. Fold changes (FC) were calculated as the ratio of medians between groups. The pasteurization effect on the HM lipidome was studied with the web-based ontology enrichment tool for lipidomic analysis: Lipid Ontology analysis - LION (www.lipidontology.com) (Molenaar et al., 2019). As an input, peak areas of annotated features in HM samples were used. The "ranking mode" with log_2FC values as local statistic and a two-tailed alternative hypothesis testing was employed.

To uncover molecular alterations caused by HoP, an integrative analysis of untargeted lipidomic and metabolomic data was carried out with the network-based Prize-collecting Steiner forest algorithm for integrative analysis of untargeted metabolomics (PIUMet) (http://fraenkel-nsf.csbi.mit.edu/piumet2/) (Pirhaji et al., 2016). As an input, *m/z* features with *p*-values < 0.01 from a Wilcoxon signed-rank test of peak areas between pre- and post-pasteurized samples were introduced either as metabolomic or lipidomic peaks, also using the -log(*p*-value) as prize to each input data point.

Data availability. Peak tables extracted from HM UPLC-QqTOF-MS analysis are accessible via the Mendeley Data repository at https://data.mendeley.com/datasets/fnzbxmkv83/1 (lipidomics) and https://data.mendeley.com/datasets/jymtst88jm/1 (metabolomics). Supplementary Table S2 summarizes FAME concentrations in all samples before and after pasteurization.

3. Results & discussion

3.1. Compositional and functional alteration of pasteurized vs raw DHM samples

Lipidomic profiles of DHM samples were acquired by UPLC-QqTOF-MS retrieving a total of 7109 metabolic features after peak detection, deconvolution, integration, alignment, within-batch effect correction, and clean-up. In total, 786 (11%) of all features were annotated. The classes with the largest numbers of annotated lipids were triradylglycerols (TGs) and diradylglycerols (DGs) followed by alkenyl-DGs and ceramides (see Fig. 1, left). 3259 features (45.8% of the total) had significantly different mean values (*t*-test, FDR-adjusted *p*-value < 0.05) and $|\log_2(FC)|>1$, including 289 (9%) annotated features using spectral libraries and MetDNA. The sub-class distribution depicted in Fig. 1 (right) shows that lipid levels across multiple lipid classes were affected by pasteurization, including DGs and TGs, alkenyl-DGs, and linoleic acids and derivatives, among others. Interestingly, 83% of DGs were affected by pasteurization while only 13% of TGs changed. In addition, it must be highlighted that, although the UPLC-QqTOF-MS method was specifically tailored to the detection of lipids, the use of a single-phase extraction procedure in combination with an untargeted detection allowed the detection of compounds from non-lipid classes such as amino acids, peptides, and analogues, and carbohydrates and carbohydrate conjugates.

Lipidomic network analysis was employed for a functional interpretation of the observed changes in the lipidomic profiles within relevant networks using the *mummichog* algorithm (Li et al., 2013). Pathway analysis detected 14 pathways with at least two significantly altered metabolites in DHM samples collected before and after pasteurization. Results summarized in Table 1 indicate a significant impact (*p*-values < 0.05) on metabolites included in the steroid hormone biosynthesis, glycosylphosphatidylinositol (GPI)-anchor biosynthesis, linoleic acid metabolism, biosynthesis of unsaturated fatty acids, and mucin type O-glycan biosynthesis pathways.

Table 1
Altered pathways in DHM linked to the pasteurization process.

Pathway name	Hits (total)	Hits (sig.)	*p*-value
Steroid hormone biosynthesis	6	4	0.02
Glycosylphosphatidylinositol (GPI)-anchor biosynthesis	4	3	0.03
Linoleic acid metabolism	7	4	0.03
Biosynthesis of unsaturated fatty acids	17	7	0.04
Mucin type O-glycan biosynthesis	2	2	0.04

Note: *p*-values from Fisher's exact *t*-test; only detected pathways with at least 2 significantly altered features are reported.

Between group comparison of the features' intensities found in the dataset, that corresponded to KEGG compounds and KEGG glycans of each altered pathway (i.e., pre-pasteurization *vs* post-pasteurization) revealed significantly different mean values (FDR-adjusted *p*-value < 0.05) and $|\log_2(FC)|>1$. Remarkably, for all features in all altered pathways, higher intensities were detected in DHM samples before pasteurization compared with DHM samples after pasteurization, except for (4Z,7Z,10Z,13Z,16Z,19Z)-Docosahexaenoyl-CoA (KEGG ID C16169, *m/z*-RT: 1146.3436–7.36) in the biosynthesis of unsaturated fatty acids pathway. The results are summarized in Supplementary Table S3 and Supplementary Figs. S1–S5.

Metabolic analysis of DHM samples retrieved a total of 466 and 379 metabolic features in the ESI^+ and ESI^- mode, respectively, after peak detection, deconvolution, integration, alignment, within-batch effect correction, and clean-up.

Fig. 2 shows the resulting network for the joint analysis of lipidomic (1033 features with *p*-value < 0.01; Wilcoxon signed-rank test) and metabolomic (35 features with *p*-value < 0.01; Wilcoxon signed-rank test) data (Pirhaji et al., 2016), in which the relation between detected features and hidden metabolites and proteins is displayed. Several features associated to the steroid hormone biosynthesis (i.e., tetrahydrocortisol, tetrahydrocorticosterone, 7a-hydroxydehydroepiandrosterone, tetrahydrodeoxycorticosterone) and the biosynthesis of unsaturated fatty acids (i.e., palmitic acid, eicosapentaenoic acid) were identified, in agreement with results shown in Table 1 and Supplementary Table S3. In addition, several metabolites associated to the steroid biosynthesis (i.e., 4,4-dimethylcholesta-8,14,24-trienol, 5-dehydroavenasterol, 7-dehydrodesmosterol, 7-dehydrocholesterol, lathosterol) and purine metabolism (i.e., guanosine, adenine, hypoxanthine, deoxyguanosine) pathways were significantly altered.

A recent study of the impact of the type of nutrition on the urinary metabolome of preterm infants has shown a significant alteration of the steroid hormone biosynthesis pathway associated to the intake of fresh

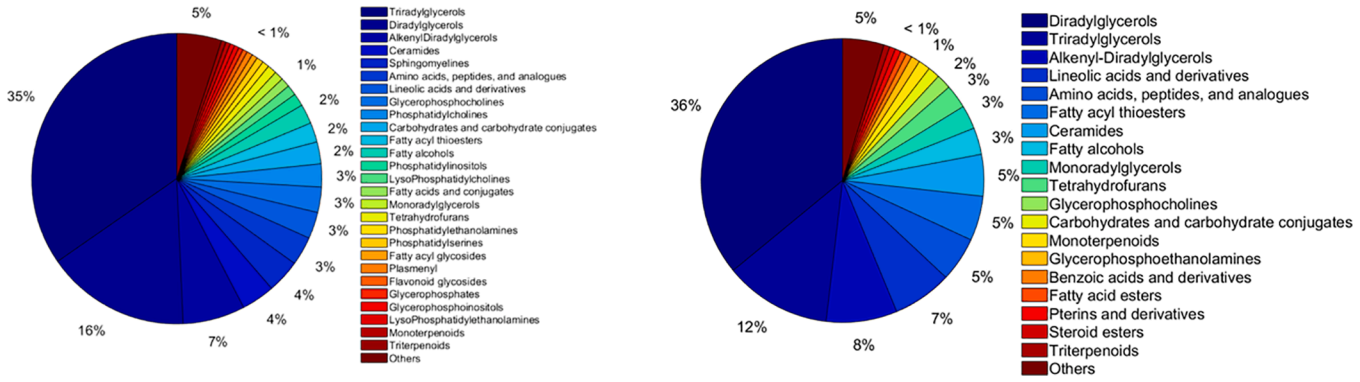

Fig. 1. Distribution by sub-classes of the metabolites annotated using HMDB/METLIN or LipidBlast spectral libraries and MetDNA detected in HM (left) and with significantly different mean values (*t*-test, FDR-adjusted p-value < 0.05) and |log2(FC)| >1 before and after pasteurization (right).

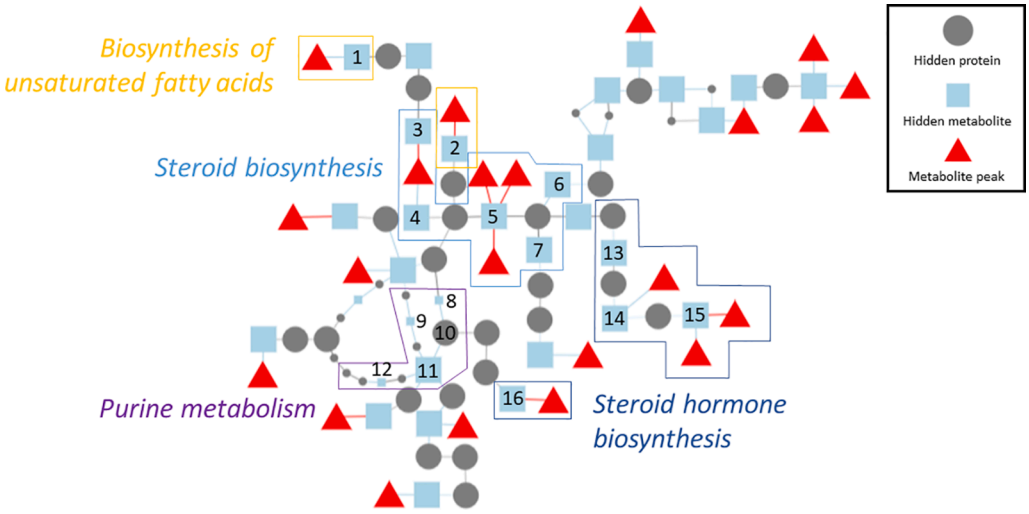

Fig. 2. PIUMet network showing metabolic pathways altered by pasteurization. Note: Pathways were highlighted if three or more hidden metabolites from the same pathway were interconnected as well as pathways those that were identified earlier by pathway analysis shown in Table 1 (biosynthesis of unsaturated fatty acids). Hidden metabolite / hidden protein #1: Palmitic acid; #2: Eicosapentaenoic acid; #3: 4,4-Dimethylcholesta-8,14,24-trienal; #4: 5-Dehydroavenasterol; #5: 7-Dehydrodesmosterol; #6: 7-Dehydrocholesterol; #7: Lathosterol; #8: Deoxyguanosine; #9: Guanosine; #10: purine nucleoside phosphorylase (PNP) protein; #11: Adenine; #11: Hypoxanthine; #12: 7a-Hydroxydehydroepiandrosterone; #13: Tetrahydrocorticosterone; #14: Tetrahydrocortisol; #15: Tetrahydrodeoxy corticosterone.

OMM or pasteurized DHM (Piñeiro-Ramos et al., 2021). This result suggested either that those steroid hormones present in HM may have a significant influence in the activity of the steroid hormone biosynthesis pathway in preterm infants, either directly or via the modification of gut-microbiota crosstalk, or that ingested levels of those compounds differ between pasteurized and fresh HM. In the present study, we focused on the analysis of DHM samples before and after HoP. Previous results found no significant differences of the levels of cortisol and cortisone in HM before and after HoP (van der Voorn et al., 2017). However, in the present study, the alteration of structurally closely related compounds included in the steroid and steroid hormone biosynthesis pathways upon pasteurization was identified (see Table 1 and Fig. 2).

The variation of total fat and fatty acid composition upon pasteurization has been studied but there is considerable variation in the reported effects (Nessel, Khashu, & Dyall, 2019). A recent review on this topic concluded that the total fat content and total fatty acid composition of expressed HM was not generally influenced by storage and handling process as most changes were found below 10% and within the expected random methodological variation (Gao et al., 2019). On the contrary, in a recent study with more than four hundred DHM samples, Piemontese et al. (Piemontese et al., 2019) confirmed that pasteurization reduced macronutrient composition, especially in terms of lipids and protein. Vincent et al. (Vincent et al., 2020) attributed these differences to the adherence of disrupted milk fat globules to container surfaces and to whether thermal treatment took place in a laboratory environment or in industrial pasteurizers routinely used in HM banks. Thus, Fidler *et al.* (Fidler, Sauerwald, Koletzko, & Demmelmair, 1998) did not find significant changes of fatty acids in HM after HoP, but a trend toward slightly lower percentage values of some fatty acids, including eicosapentaenoic acid was found. This observation was in agreement with the results from PIUMet network analysis presented in this study (see Fig. 2).

Furthermore, alterations of the purine metabolism were detected. A significant increase in nucleotide monophosphates associated to HoP of HM, which could be produced from the break-down of polymeric nucleotides and/or nucleotide adducts was reported (Mateos-Vivas et al., 2015). Here, we observed changes in guanosine and deoxyguanosine, which participate as building blocks in the synthesis of oligonucleotides. In addition, in the network-based approach, the purine nucleoside phosphorylase (PNP) protein, which catalyses the phosphorolytic breakdown of the *N*-glycosidic bond in the beta-(deoxy)ribonucleoside molecules, with the formation of the corresponding free purine bases and pentose-1-phosphate, appeared altered (see Fig. 2).

Finally, no literature reports regarding changes of glycans in pasteurized HM have been found. Although HM oligosaccharides (HMOs) are reported to be unaffected by HoP (Hahn, Kim, Song, Park, & Kang, 2019), in this work, mucin type *O*-glycans appeared altered upon pasteurization. As for HMOs, it has been hypothesized that mucin type *O*-glycans may have a certain role in mucus barrier function by promoting mutualism with host microbiota (Bergstrom & Xia, 2013). Hence, additional studies on specific glycans are needed.

In the lipid ontology enrichment analysis performed in pursuit of functional alterations of the lipidomic profile of HM after pasteurization, 634 out of 786 (80.66%) annotated features were matched to LION entries. The LION enrichment graph with the four major branches (lipid classification, chemical and physical properties, function, and subcellular component) is shown in Fig. 3.

The terms “lipid droplet” and “lipid storage”, belonging to the category “sub-cellular component” and “function”, respectively, were enriched in pasteurized DHM. Inspection of the lipid species responsible of these LION-terms revealed the presence of TGs. It has been described that the heating process very likely causes the disruption of the fat globule membranes. In fact, a significant decreased in fat globule size and, hence, an increase in the overall surface area upon pasteurization have been previously reported (Lopez, Cauty, & Guyomarc’h, 2015). This surface increase of the TG/water interface jointly with potential changes in the interface composition might play an important role with respect to chemical and enzymatic reactions that take place at the interface. In this work, the terms “membrane component” and “lipid-mediated signaling”, belonging to the ontology root “function”, were down-regulated by pasteurization. The first term is associated with lipids primarily regarded as structural components of lipid bilayers (i.e., DGs, glycerophosphocholines, phosphosphingolipids, and lyso-glycerophospholipids (GPs)) indicating a decay of membrane lipids during pasteurization. In this study, a total of 258 identifiers were ascribed to this LION-term, distributed as DGs (59%), GPs (24%), sphingomyelins (12%), and lyso-GPs (5%). The term “lipid-mediated signaling”, associated with lipids implicated in signaling, such as DGs, monoradylglycerols, and lyso-GPs, was also down-regulated because of processing. Changes in the oxylipin composition during HoP have been previously observed (Pitino et al., 2019). This potential functional alteration should be addressed in future studies, as it could potentially be important for cellular processes, and especially relevant for the brain development of preterm infants. Lipids related to the term “negative intrinsic curvature” were downregulated in pasteurized DHM. LION assumes curvature to be predominantly head-group-dependent and neglects fatty acid composition. In this work, 184 identifiers, distributed in

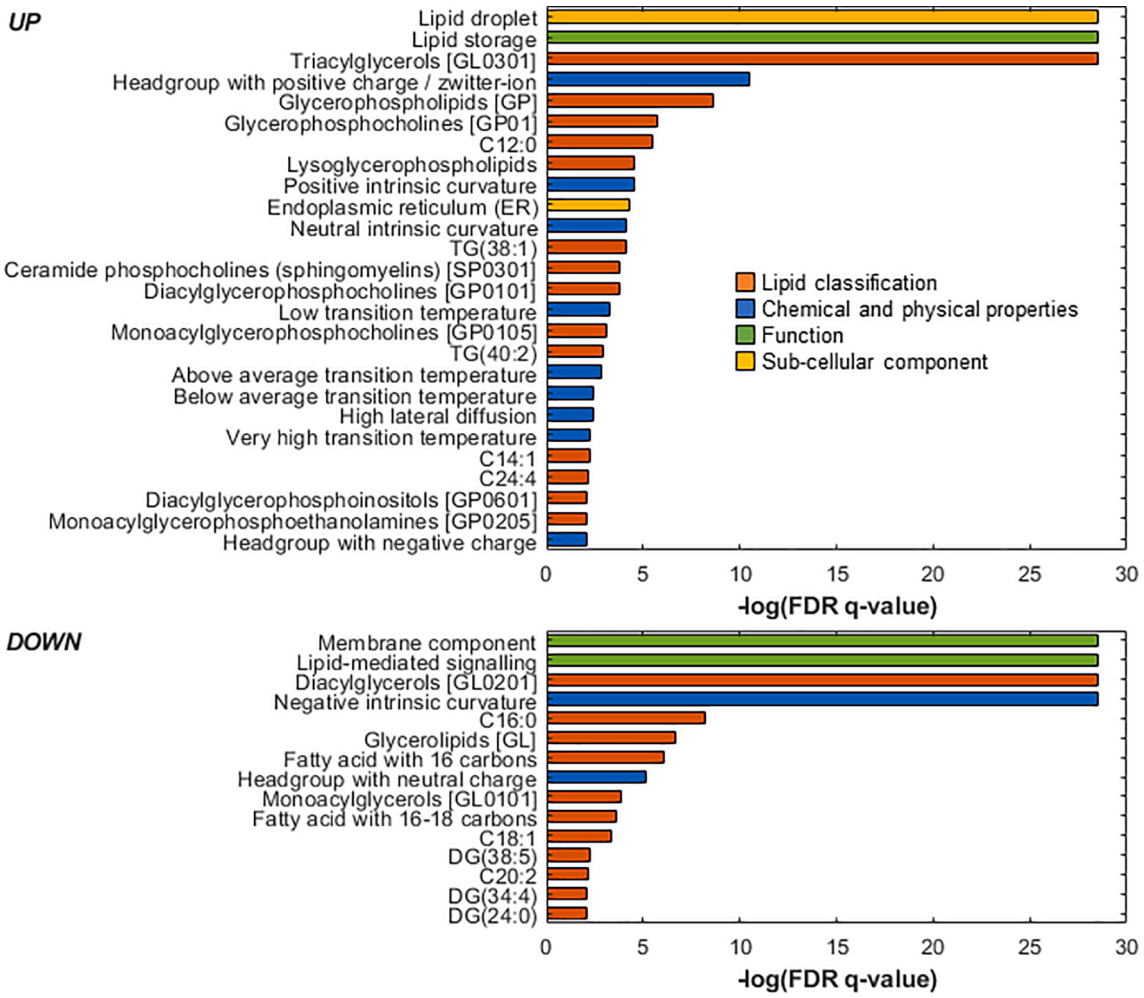

Fig. 3. Lipid ontology enrichment analysis of the pasteurization process performed in the "ranking mode" (DHM-Post *vs* DHM-Pre). Only the 40 most enriched LION-term have been represented.

DGs (80%), ceramides (15%) and GPs (4%), were ascribed to this term indicating a change in physico-chemical properties of HM upon pasteurization.

Lipid ontology enrichment analysis underpinned the alteration of different lipid classes upon pasteurization as discussed earlier (see also Fig. 1). In addition, it allowed to draw conclusions regarding the consequences of those changes that were associated to the physical and chemical properties (i.e., negative intrinsic curvature), sub-cellular components (i.e., lipid droplet) and function (i.e., lipid storage, membrane component, and lipid-mediated signaling) of altered lipids.

3.2. Fatty acid analysis

A method for the quantification of derivatized free fatty acids after acidic hydrolysis of lipids in HM was developed and validated following the FDA guidelines for bioanalytical method validation. Supplementary Table S4 summarizes the employed concentration intervals, which were selected considering the wide expected inter- and intra-individual variability. Intra and inter-day accuracy and precision of the method varied between 80% and 121%, and 1.0% and 20%, respectively, in standards and between 80% and 122%, and 1.0% and 14%, respectively, in spiked samples. Selectivity was confirmed and no carry-over was detected.

A total of 29 fatty acids from the 36 fatty acids included in the analytical method were found at higher levels than the lower limit of quantification and were successfully quantified in HM samples. Mean concentrations of five fatty acids were unaffected by pasteurization, two fatty acids showed an increase, and 22 fatty acids showed a statistically significant decrease (median decrease 10% (14% IQR)) (see Table 2).

Besides, the relative decrease in the concentration was higher for saturated fatty acids (SFAs) (25%), followed by polyunsaturated fatty acids (PUFAs) (18%), long-chain fatty acids (LCFAs) (15%), and monounsaturated fatty acids (MUFAs) (12%) (see Fig. 4).

The observed reduction in the fatty acids concentrations was in agreement with previous results (Gao et al., 2019). The small decrease in concentration found in this work might be, at least partially, responsible for the controversy in literature reports (Nessel et al., 2019) on the effect of pasteurization on fatty acid concentration in HM and underlines the importance of method validation for enabling the detection of subtle changes between groups.

4. Conclusions

This study provides the first comprehensive assessment of the impact of pasteurization on the HM lipidome and metabolome. Results identified affected metabolites that were related to steroids (i.e., steroid

Table 2
Individual and total content of fatty acids in DHM samples before (DHM-Pre) and after (DHM-Post) pasteurization.

Fatty acid	Median (IQR) (mM)		*p*-value
	DHM-Pre	DHM-Post	
Hexanoate (C6:0)	56 (20–95)	35 (18–75)	0.0002
Octanoate (C8:0)	41 (19–55)	29 (11–47)	0.0005
Decanoate (C10:0)	42 (22–53)	35 (15–45)	0.0002
Undecanoate (C11)	< LOQ	< LOQ	–
Laurate (C12:0)	14 (10–18)	10 (9–16)	0.02
Tridecanoate	< LOQ	< LOQ	–
Myristate (C14:0)	4 (3–4)	3 (2–4)	0.013
Myristoleate (C14:1)	0.10 (0.06–0.15)	0.08 (0.05–0.14)	0.0005
Pentadecanoate (C15:0)	0.10 (0.08–0.14)	0.09 (0.06–0.13)	0.0007
cis-10-Pentadecenoic (C15:1)	< LOQ	< LOQ	–
Palmitate (C16:0)	9 (7–10)	8 (5–10)	0.0005
Palmitoleate (C16:1)	0.9 (0.6–1.2)	0.9 (0.5–1.0)	0.0012
Heptadecanoate (C17:0)	0.3 (0.2–0.3)	0.3 (0.2–0.3)	0.003
cis-10-Heptadecenoic (C17:1)	0.2 (0.15–0.3)	0.2 (0.14–0.2)	0.0002
Stearate (C18:0)	3 (2–5)	3 (3–4)	0.0002
Oleic (C18:1n9c)	30 (26–35)	26 (18–30)	0.002
Elaidic (C18:1n9t)	0.8 (0.7–1.0)	0.8 (0.5–0.9)	0.013
Linoleic (C18:2n6c)	6 (5–8)	5 (4–7)	0.0002
Linolelaidic (C18:2n6t)	5 (1.1–8)	4 (0.8–7)	0.0007
gamma-Linolenic (C18:3n6)	0.2 (0.15–0.3)	0.2 (0.15–0.2)	0.0012
Linolenic (C18:3n3)	0.4 (0.4–0.5)	0.4 (0.3–0.4)	0.0002
Eicosanoic (C20:0)	0.3 (0.3–0.3)	0.3 (0.3–0.3)	0.02
cis-11-Eicosenoic (C20:1)	0.2 (0.13–0.2)	0.15 (0.13–0.2)	0.02
cis-11,14-Eicosadienoic (C20:2)	0.09 (0.05–0.2)	0.07 (0.04–0.2)	0.02
cis-8,11,14-Eicosatrienoic (C20:3n6)	0.4 (0.3–0.5)	0.4 (0.3–0.4)	0.05
Arachidonic (C20:4n6)	0.3 (0.3–0.4)	0.3 (0.3–0.4)	0.002
Heneicosanoate (C21:0)	< LOQ	< LOQ	–
cis-11,14,17-Eicosatrienoic (C20:3n3)	0.15 (0.11–0.2)	0.15 (0.11–0.2)	0.13
cis-5,8,11,14,17-Eicosapentaenoic (C20:5n3)	< LOQ	< LOQ	–
Docosanoate (C22:0)	0.5 (0.4–0.5)	0.5 (0.4–0.5)	0.02
Erucic acid (C22:1)	0.006 (0.005–0.13)	0.007 (0.004–0.13)	0.13
cis-13,16-Docosadienoic (C22:2)	0.3 (0.2–0.3)	0.3 (0.2–0.3)	0.5
Tricosanoate (C23:0)	< LOQ	< LOQ	–
cis-4,7,10,13,16,19-Docosahexaenoic (C22:6n3)	0.5 (0.4–0.7)	0.5 (0.4–0.6)	0.008
Lignocerate (C24:0)	0.2 (0.2–0.3)	0.2 (0.2–0.3)	0.05
Nervonic acid (C24:1)	< LOQ	< LOQ	–
TOTAL	230 (120–290)	169 (104–252)	0.0002

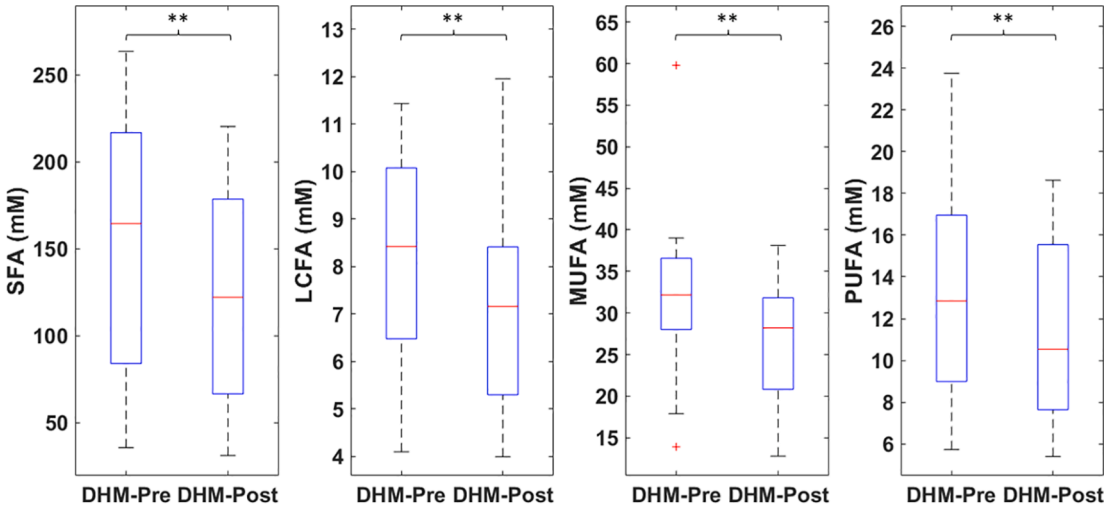

Fig. 4. Total saturated fatty acids (SFA), long chain fatty acids (LCFA), monounsaturated fatty acids (MUFA) and polyunsaturated fatty acids (PUFA) of DHM-samples before (DHM-Pre) and after (DHM-Post) pasteurization. ***p*-value < 0.01, one-tailed Wilcoxon signed-rank test.

biosynthesis and steroid hormone biosynthesis) as well as fatty acids (i.e., biosynthesis of unsaturated fatty acids and linoleic acid metabolism) metabolic pathways. Earlier studies solely focusing on cortisone and cortisol did not find alterations due to HoP. In this work, however, the levels of structurally related metabolites were affected by the thermal treatment. The present work furthermore demonstrates that HoP has an impact not only on the composition, but also on the physico-chemical properties, cellular components, and the functionality of lipids. Finally, the concentrations of the 76% of the analyzed fatty acids were altered after pasteurization, with a median decrease in the relative concentration of 10%. Results obtained encourage further research into the analysis of the biological relevance and impact of the observed changes in composition and functionality of HM components.

5. Funding sources

This work was supported by the *Instituto de Salud Carlos III*, Spain [grant numbers CD19/00176 and CP16/00034]; the Ministry of Science and Innovation, Spain [grant number IJC2018-036209-I], *Generalitat Valenciana* [project number GV/2021/186], and the European Union's Horizon 2020 Research and Innovation Programme through the Nutrishield project (https://nutrishield-project.eu/) [Grant Agreement No 818110].

CRediT authorship contribution statement

Isabel Ten-Doménech: Conceptualization, Supervision, Funding acquisition, Visualization, Writing – original draft, Software, Data curation, Formal analysis, Validation, Investigation, Methodology, Writing – review & editing. **Victoria Ramos-Garcia:** Visualization, Writing – original draft, Software, Data curation, Formal analysis, Validation, Investigation, Methodology, Writing – review & editing. **Marta Moreno-Torres:** Investigation, Methodology, Writing – review & editing. **Anna Parra-Llorca:** Software, Data curation, Formal analysis, Validation, Investigation, Methodology, Writing – review & editing. **María Gormaz:** Conceptualization, Supervision, Funding acquisition, Investigation, Methodology, Writing – review & editing. **Máximo Vento:** Conceptualization, Supervision, Funding acquisition, Investigation, Methodology, Writing – review & editing. **Julia Kuligowski:** Conceptualization, Supervision, Funding acquisition, Visualization, Writing – original draft, Software, Data curation, Formal analysis, Validation, Investigation, Methodology, Writing – review & editing. **Guillermo Quintás:** Conceptualization, Supervision, Funding acquisition, Software, Data curation, Formal analysis, Validation, Investigation, Methodology, Writing – review & editing.

Declaration of Competing Interest

The authors declare that they have no known competing financial interests or personal relationships that could have appeared to influence the work reported in this paper.

Appendix A. Supplementary data

Supplementary data to this article can be found online at https://doi.org/10.1016/j.foodchem.2022.132581.

References

Bergstrom, K. S. B., & Xia, L. (2013). Mucin-type O-glycans and their roles in intestinal homeostasis. *Glycobiology, 23*(9), 1026–1037. https://doi.org/10.1093/glycob/cwt045

Boquien, C.-Y. (2018). Human Milk: An Ideal Food for Nutrition of Preterm Newborn. *Frontiers in Pediatrics, 6*. https://doi.org/10.3389/fped.2018.00295

Broadhurst, D., Goodacre, R., Reinke, S. N., Kuligowski, J., Wilson, I. D., Lewis, M. R., & Dunn, W. B. (2018). Guidelines and considerations for the use of system suitability and quality control samples in mass spectrometry assays applied in untargeted clinical metabolomic studies. *Metabolomics, 14*(6), 72. https://doi.org/10.1007/s11306-018-1367-3

Caspi, R., Billington, R., Ferrer, L., Foerster, H., Fulcher, C. A., Keseler, I. M., … Karp, P. D. (2016). The MetaCyc database of metabolic pathways and enzymes and the BioCyc collection of pathway/genome databases. *Nucleic Acids Research, 44*(D1), D471–D480. https://doi.org/10.1093/nar/gkv1164

Chang, C. -C., & Lin, C. -J. (2011). LIBSVM: A Library for Support Vector Machines. *ACM Transactions on Intelligent Systems and Technology 2*(3), 27:1-27:27. doi:10.1145/1961189.1961199.

Chong, J., Soufan, O., Li, C., Caraus, I., Li, S., Bourque, G., … Xia, J. (2018). MetaboAnalyst 4.0: Towards more transparent and integrative metabolomics analysis. *Nucleic Acids Research, 46*(W1), W486–W494. https://doi.org/10.1093/nar/gky310

Colaizy, T. T. (2021). Effects of milk banking procedures on nutritional and bioactive components of donor human milk. *Seminars in Perinatology, 45*(2), Article 151382. https://doi.org/10.1016/j.semperi.2020.151382

Cruz-Hernandez, C., Goeuriot, S., Giuffrida, F., Thakkar, S. K., & Destaillats, F. (2013). Direct quantification of fatty acids in human milk by gas chromatography. *Journal of Chromatography A, 1284*, 174–179. https://doi.org/10.1016/j.chroma.2013.01.094

Fidler, N., Sauerwald, T. U., Koletzko, B., & Demmelmair, H. (1998). Effects of Human Milk Pasteurization and Sterilization on Available Fat Content and Fatty Acid Composition. *Journal of Pediatric Gastroenterology and Nutrition, 27*(3), 317–322.

Food and Drug Administration (FDA). Guidance for Industry: Bioanalytical Method Validation. Food and Drug Administration, Center for Drug Evaluation and Research, Center for Veterinary Medicine. (2018). 44.

Gao, C., Miller, J., Middleton, P. F., Huang, Y.-C., McPhee, A. J., & Gibson, R. A. (2019). Changes to breast milk fatty acid composition during storage, handling and processing: A systematic review. *Prostaglandins, Leukotrienes, and Essential Fatty Acids, 146*, 1–10. https://doi.org/10.1016/j.plefa.2019.04.008

Hahn, W.-H., Kim, J., Song, S., Park, S., & Kang, N. M. (2019). The human milk oligosaccharides are not affected by pasteurization and freeze-drying. *The Journal of Maternal-Fetal & Neonatal Medicine: The Official Journal of the European Association of Perinatal Medicine, the Federation of Asia and Oceania Perinatal Societies, the International Society of Perinatal Obstetricians, 32*(6), 985–991. https://doi.org/10.1080/14767058.2017.1397122

Horta, D., Moreno-Torres, M., Ramírez-Lázaro, M. J., Lario, S., Kuligowski, J., Sanjuan-Herráez, J. D., … Calvet, X. (2020). Analysis of the Association between Fatigue and the Plasma Lipidomic Profile of Inflammatory Bowel Disease Patients. *Journal of Proteome Research*. https://doi.org/10.1021/acs.jproteome.0c00462

Hutchins, P. D., Russell, J. D., & Coon, J. J. (2018). LipiDex: An Integrated Software Package for High-Confidence Lipid Identification. *Cell Systems, 6*(5), 621–625.e5. https://doi.org/10.1016/j.cels.2018.03.011

Kessner, D., Chambers, M., Burke, R., Agus, D., & Mallick, P. (2008). ProteoWizard: Open source software for rapid proteomics tools development. *Bioinformatics (Oxford, England), 24*(21), 2534–2536. https://doi.org/10.1093/bioinformatics/btn323

Kuhl, C., Tautenhahn, R., Böttcher, C., Larson, T. R., & Neumann, S. (2012). CAMERA: An Integrated Strategy for Compound Spectra Extraction and Annotation of Liquid Chromatography/Mass Spectrometry Data Sets. *Analytical Chemistry, 84*(1), 283–289. https://doi.org/10.1021/ac202450g

Kuligowski, J., Sánchez-Illana, Á., Sanjuán-Herráez, D., Vento, M., & Quintás, G. (2015). Intra-batch effect correction in liquid chromatography-mass spectrometry using quality control samples and support vector regression (QC-SVRC). *The Analyst, 140*(22), 7810–7817. https://doi.org/10.1039/c5an01638j

Li, S., Park, Y., Duraisingham, S., Strobel, F. H., Khan, N., Soltow, Q. A., … Pulendran, B. (2013). Predicting Network Activity from High Throughput Metabolomics. *PLoS Computational Biology, 9*(7). https://doi.org/10.1371/journal.pcbi.1003123

Lopez, C., Cauty, C., & Guyomarc'h, F. (2015). Organization of lipids in milks, infant milk formulas and various dairy products: Role of technological processes and potential impacts. *Dairy Science & Technology, 95*(6), 863–893. https://doi.org/10.1007/s13594-015-0263-0

Martínez-Sena, T., Luongo, G., Sanjuan-Herráez, D., Castell, J. V., Vento, M., Quintás, G., & Kuligowski, J. (2019). Monitoring of system conditioning after blank injections in untargeted UPLC-MS metabolomic analysis. *Scientific Reports, 9*(1), 1–9. https://doi.org/10.1038/s41598-019-46371-w

Mateos-Vivas, M., Rodríguez-Gonzalo, E., Domínguez-Álvarez, J., García-Gómez, D., Ramírez-Bernabé, R., & Carabias-Martínez, R. (2015). Analysis of free nucleotide monophosphates in human milk and effect of pasteurisation or high-pressure processing on their contents by capillary electrophoresis coupled to mass spectrometry. *Food Chemistry, 174*, 348–355. https://doi.org/10.1016/j.foodchem.2014.11.051

Miller, J., Tonkin, E., Damarell, R. A., McPhee, A. J., Suganuma, M., Suganuma, H., … Collins, C. T. (2018). A Systematic Review and Meta-Analysis of Human Milk Feeding and Morbidity in Very Low Birth Weight Infants. *Nutrients, 10*(6), 707. https://doi.org/10.3390/nu10060707

Molenaar, M. R., Jeucken, A., Wassenaar, T. A., van de Lest, C. H. A., Brouwers, J. F., & Helms, J. B. (2019). LION/web: A web-based ontology enrichment tool for lipidomic data analysis. *GigaScience, 8*(6). https://doi.org/10.1093/gigascience/giz061

Nessel, I., Khashu, M., & Dyall, S. C. (2019). The effects of storage conditions on long-chain polyunsaturated fatty acids, lipid mediators, and antioxidants in donor human milk—A review. *Prostaglandins, Leukotrienes, and Essential Fatty Acids, 149*, 8–17. https://doi.org/10.1016/j.plefa.2019.07.009

Parra-Llorca, A., Gormaz, M., Alcántara, C., Cernada, M., Nuñez-Ramiro, A., Vento, M., & Collado, M. C. (2018). Preterm Gut Microbiome Depending on Feeding Type: Significance of Donor Human Milk. *Frontiers in Microbiology, 9*. https://doi.org/10.3389/fmicb.2018.01376

Parra-Llorca, A., Gormaz, M., Sánchez-Illana, Á., Piñeiro-Ramos, J. D., Collado, M. C., Serna, E., … Vento, M. (2019). Does pasteurized donor human milk efficiently protect preterm infants against oxidative stress? *Antioxidants & Redox Signaling*. https://doi.org/10.1089/ars.2019.7821

Piemontese, P., Mallardi, D., Liotto, N., Tabasso, C., Menis, C., Perrone, M., … Mosca, F. (2019). Macronutrient content of pooled donor human milk before and after Holder pasteurization. *BMC Pediatrics, 19*(1), 58. https://doi.org/10.1186/s12887-019-1427-5

Piñeiro-Ramos, J. D., Parra-Llorca, A., Ten-Doménech, I., Gormaz, M., Ramón-Beltrán, A., Cernada, M., … Vento, M. (2021). Effect of donor human milk on host-gut microbiota and metabolic interactions in preterm infants. *Clinical Nutrition (Edinburgh, Scotland), 40*(3), 1296–1309. https://doi.org/10.1016/j.clnu.2020.08.013

Pirhaji, L., Milani, P., Leidl, M., Curran, T., Avila-Pacheco, J., Clish, C. B., … Fraenkel, E. (2016). Revealing disease-associated pathways by network integration of untargeted metabolomics. *Nature Methods, 13*(9), 770–776. https://doi.org/10.1038/nmeth.3940

Pitino, M. A., Alashmali, S. M., Hopperton, K. E., Unger, S., Pouliot, Y., Doyen, A., … Bazinet, R. P. (2019). Oxylipin concentration, but not fatty acid composition, is altered in human donor milk pasteurised using both thermal and non-thermal techniques. *The British Journal of Nutrition, 122*(1), 47–55. https://doi.org/10.1017/S0007114519000916

Poulimeneas, D., Bathrellou, E., Antonogeorgos, G., Mamalaki, E., Kouvari, M., Kuligowski, J., … NUTRISHIELD Consortium. (2021). Feeding the preterm infant: An overview of the evidence. *International Journal of Food Sciences and Nutrition, 72*(1), 4–13. https://doi.org/10.1080/09637486.2020.1754352

Quigley, M., Embleton, N. D., & McGuire, W. (2019). Formula versus donor breast milk for feeding preterm or low birth weight infants. *The. Cochrane Database of Systematic Reviews, 7*, CD002971. https://doi.org/10.1002/14651858.CD002971.pub5

Shen, X., Wang, R., Xiong, X., Yin, Y., Cai, Y., Ma, Z., … Zhu, Z.-J. (2019). Metabolic reaction network-based recursive metabolite annotation for untargeted metabolomics. *Nature Communications, 10*(1), 1516. https://doi.org/10.1038/s41467-019-09550-x

Tautenhahn, R., Patti, G. J., Rinehart, D., & Siuzdak, G. (2012). XCMS Online: A Web-Based Platform to Process Untargeted Metabolomic Data. *Anal. Chem., 84*(11), 5035–5039.

Ten-Doménech, I., Martínez-Sena, T., Moreno-Torres, M., Sanjuan-Herráez, J. D., Castell, J. V., Parra-Llorca, A., … Kuligowski, J. (2020). Comparing Targeted vs. Untargeted MS2 Data-Dependent Acquisition for Peak Annotation in LC–MS Metabolomics. *Metabolites, 10*(4), 126. https://doi.org/10.3390/metabo10040126

van der Voorn, B., de Waard, M., Dijkstra, L. R., Heijboer, A. C., Rotteveel, J., van Goudoever, J. B., & Finken, M. J. J. (2017). Stability of Cortisol and Cortisone in Human Breast Milk During Holder Pasteurization. *Journal of Pediatric Gastroenterology and Nutrition, 65*(6), 658–660. https://doi.org/10.1097/MPG.0000000000001678

Villaseñor, A., Garcia-Perez, I., Garcia, A., Posma, J. M., Fernández-López, M., Nicholas, A. J., … Barbas, C. (2014). Breast milk metabolome characterization in a single-phase extraction, multiplatform analytical approach. *Analytical Chemistry, 86*(16), 8245–8252. https://doi.org/10.1021/ac501853d

Vincent, M., Ménard, O., Etienne, J., Ossemond, J., Durand, A., Buffin, R., … Penhoat, A. (2020). Human milk pasteurisation reduces pre-lipolysis but not digestive lipolysis and moderately decreases intestinal lipid uptake in a combination of preterm infant in vitro models. *Food Chemistry, 329*, Article 126927. https://doi.org/10.1016/j.foodchem.2020.126927

Wesolowska, A., Sinkiewicz-Darol, E., Barbarska, O., Bernatowicz-Lojko, U., Borszewska-Kornacka, M. K., & van Goudoever, J. B. (2019). Innovative Techniques of Processing Human Milk to Preserve Key Components. *Nutrients, 11*(5). https://doi.org/10.3390/nu11051169

World Health Organization. (2017). *Guideline: Protecting, promoting and supporting breastfeeding in facilities providing maternity and newborn services.* http://www.ncbi.nlm.nih.gov/books/NBK487819/.